



This is the accepted manuscript made available via CHORUS. The article has been published as:

Observation of Directed Flow of Hypernuclei 
$$\langle \cos \theta_{\text{H}} \rangle \sim \frac{1}{3} \langle \cos \theta_{\text{H}} \rangle$$
 and 
$$\langle \cos \theta_{\text{H}} \rangle \sim \frac{1}{4} \langle \cos \theta_{\text{H}} \rangle$$

in 
$$\sqrt{s_{\text{NN}}} = 3 \text{ GeV}$$

math 
$$\sqrt{s_{\text{NN}}} = 3 \text{ GeV}$$

Collisions at RHIC

B. E. Aboona et al. (STAR Collaboration)

Phys. Rev. Lett. **130**, 212301 — Published 24 May 2023

DOI: [10.1103/PhysRevLett.130.212301](https://doi.org/10.1103/PhysRevLett.130.212301)

1 **First Observation of Directed Flow of Hypernuclei  ${}^3_{\Lambda}\text{H}$  and  ${}^4_{\Lambda}\text{H}$  in  $\sqrt{s_{\text{NN}}} = 3$  GeV**  
2 **Au+Au Collisions at RHIC**

3 B. E. Aboona, D. M. Anderson, Y. Liu, J. Pan, and R. E. Tribble  
4 *Texas A&M University, College Station, Texas 77843*

5 J. Adam, J. Ceska, A. Das, and O. Lomicky  
6 *Czech Technical University in Prague, FNSPE, Prague 115 19, Czech Republic*

7 J. R. Adams, J. D. Brandenburg, T. J. Humanic, and X. Liu  
8 *Ohio State University, Columbus, Ohio 43210*

9 G. Agakishiev, A. Aitbaev, A. Aparin, G. S. Averichev, T. G. Dedovich,  
10 A. Kechechyan, A. A. Korobitsin, R. Lednicky, V. B. Luong, A. Mudrokh,  
11 Y. Panebratsev, O. V. Rogachevsky, E. Shahaliev, M. V. Tokarev, and S. Vokal  
12 *Joint Institute for Nuclear Research, Dubna 141 980*

13 I. Aggarwal, M. M. Aggarwal, A. Dhamija, L. Kumar, A. S. Nain, N. K. Pruthi, and J. Singh  
14 *Panjab University, Chandigarh 160014, India*

15 Z. Ahammed  
16 *Variable Energy Cyclotron Centre, Kolkata 700064, India*

17 I. Alekseev  
18 *Alikhanov Institute for Theoretical and Experimental Physics NRC "Kurchatov Institute", Moscow 117218 and*  
19 *National Research Nuclear University MEPhI, Moscow 115409*

20 J. Atchison, M. Daugherty, J. L. Drachenberg, and D. Isenhower  
21 *Abilene Christian University, Abilene, Texas 79699*

22 V. Bairathi and S. Kabana  
23 *Instituto de Alta Investigación, Universidad de Tarapacá, Arica 1000000, Chile*

24 W. Baker, K. Barish, D. Chen, M. L. Kabir, D. Kapukchyan, X. Liang, E. Loyd, A. Paul, C. Racz, R. Seto, and Y. Wu  
25 *University of California, Riverside, California 92521*

26 J. G. Ball Cap  
27 *University of Houston, Houston, Texas 77204*

28 P. Bhagat, A. Bhasin, A. Gupta, A. Jalotra, and M. Sharma  
29 *University of Jammu, Jammu 180001, India*

30 S. Bhatta, S. L. Huang, R. Lacey, N. Magdy, C. Sun, Z. Yan, and C. Zhang  
31 *State University of New York, Stony Brook, New York 11794*

32 I. G. Bordyuzhin, E. Samigullin, and D. N. Svirida  
33 *Alikhanov Institute for Theoretical and Experimental Physics NRC "Kurchatov Institute", Moscow 117218*

34 A. V. Brandin, L. Kochenda, P. Kravtsov, G. Nigmatkulov,  
35 V. A. Okorokov, P. Parfenov, M. Strikhanov, and A. Taranenko  
36 *National Research Nuclear University MEPhI, Moscow 115409*

37 X. Z. Cai and B. Xi  
38 *Shanghai Institute of Applied Physics, Chinese Academy of Sciences, Shanghai 201800*

39 H. Caines, F. A. Flor, J. W. Harris, R. Kunnawalkam Elayavalli,  
40 T. Liu, I. Mooney, D. B. Nemes, Y. Song, and A. Tamis

41 *Yale University, New Haven, Connecticut 06520*

42 M. Calderón de la Barca Sánchez, D. Cebra, M. D. Harasty, B. Kimelman, and Z. W. Sweger  
43 *University of California, Davis, California 95616*

44 I. Chakaberia, X. Dong, Y. Hu, Y. Ji, H. S. Ko, H. S. Matis,  
45 G. Odyniec, S. Oh, H. G. Ritter, J. H. Thomas, H. Wieman, and N. Xu  
46 *Lawrence Berkeley National Laboratory, Berkeley, California 94720*

47 B. K. Chan, Y. Cheng, H. Z. Huang, D. Neff, S. Trentalange, G. Wang, X. Wu, and Z. Xu  
48 *University of California, Los Angeles, California 90095*

49 Z. Chang, W. W. Jacobs, H. Liu, and S. W. Wissink  
50 *Indiana University, Bloomington, Indiana 47408*

51 J. Chen, Z. Chen, X. Gou, Y. He, C. Li, T. Lin, M. Nie, N. R. Sahoo, Y. Shi, X. Wang,  
52 Z. Wang, Q. H. Xu, Y. Xu, G. Yan, C. Yang, Q. Yang, L. Yi, Y. Yu, and J. Zhang  
53 *Shandong University, Qingdao, Shandong 266237*

54 J. H. Chen, S. Choudhury, W. He, L. Ma, Y. G. Ma, T. Shao, D. Y. Shen, Q. Y. Shou, J. Zhao, and C. Zhou  
55 *Fudan University, Shanghai, 200433*

56 J. Cheng, X. Huang, Y. Huang, K. Kang, Y. Li, Z. Qin, Y. Wang, Z. G. Xiao, and X. Zhu  
57 *Tsinghua University, Beijing 100084*

58 W. Christie, X. Chu, L. Didenko, J. C. Dunlop, O. Eyser, Y. Fisyak, K. Kauder, H. W. Ke, A. Kiselev,  
59 J. M. Landgraf, A. Lebedev, J. H. Lee, N. Lewis, T. Ljubicic, R. S. Longacre, R. Ma, A. S. Nunes,  
60 A. Ogawa, B. S. Page, R. Pak, L. Ruan, W. B. Schmidke, P. V. Shanmuganathan, A. H. Tang, P. Tribedy,  
61 Z. Tu, T. Ullrich, G. Van Buren, F. Videbæk, J. C. Webb, Z. Xu, K. Yip, Z. Zhang, and M. Zhao  
62 *Brookhaven National Laboratory, Upton, New York 11973*

63 H. J. Crawford, J. Engelage, E. G. Judd, J. M. Nelson, and C. Perkins  
64 *University of California, Berkeley, California 94720*

65 G. Dale-Gau, O. Evdokimov, T. Huang, G. Wilks, Z. Ye, and Z. Zhang  
66 *University of Illinois at Chicago, Chicago, Illinois 60607*

67 I. M. Deppner, Y. H. Leung, Y. Söhngen, and P. C. Weidenkaff  
68 *University of Heidelberg, Heidelberg 69120, Germany*

69 A. A. Derevschikov, N. G. Minaev, D. A. Morozov, and L. V. Nogach  
70 *NRC "Kurchatov Institute", Institute of High Energy Physics, Protvino 142281*

71 L. Di Carlo, M. Kelsey, W. J. Llope, G. McNamara, J. Putschke,  
72 N. Raha, D. J. Stewart, V. Verkest, and S. A. Voloshin  
73 *Wayne State University, Detroit, Michigan 48201*

74 P. Dixit, Md. Nasim, A. K. Sahoo, and N. Sharma  
75 *Indian Institute of Science Education and Research (IISER), Berhampur 760010, India*

76 E. Duckworth, D. Keane, Y. Liang, S. Margetis, S. K. Radhakrishnan, and A. I. Sheikh  
77 *Kent State University, Kent, Ohio 44242*

78 G. Eppley, F. Geurts, Y. Han, C. Jin, W. Li, I. Upsal, and Z. Ye  
79 *Rice University, Houston, Texas 77251*

80 S. Esumi, M. Isshiki, T. Niida, R. Nishitani, T. Nonaka, K. Okubo, H. Sako, S. Sato, and T. Todoroki  
81 *University of Tsukuba, Tsukuba, Ibaraki 305-8571, Japan*

82 A. Ewigleben, A. G. Knospe, T. Protzman, and C. A. Tomkiel  
83 *Lehigh University, Bethlehem, Pennsylvania 18015*

84 R. Fatemi, H. Harrison, and M. A. Rosales Aguilar  
85 *University of Kentucky, Lexington, Kentucky 40506-0055*

86 S. Fazio  
87 *University of Calabria & INFN-Cosenza, Italy*

88 C. J. Feng, H. Huang, Y. Yang, and Z. J. Zhang  
89 *National Cheng Kung University, Tainan 70101*

90 Y. Feng, C. W. Robertson, B. Srivastava, B. Stringfellow, F. Wang, and W. Xie  
91 *Purdue University, West Lafayette, Indiana 47907*

92 E. Finch  
93 *Southern Connecticut State University, New Haven, Connecticut 06515*

94 C. Fu, Y. Huang, F. Liu, H. Liu, L. Liu, Z. Liu, X. F. Luo, K. Mi, S. S. Shi,  
95 Y. Wang, J. Wu, Y. Xu, D. Zhang, Y. Zhang, S. Zhou, and Y. Zhou  
96 *Central China Normal University, Wuhan, Hubei 430079*

97 N. Ghimire, N. S. Lukow, J. D. Nam, B. R. Pokhrel, M. Posik, A. Quintero, and B. Sorrow  
98 *Temple University, Philadelphia, Pennsylvania 19122*

99 A. Gibson, D. Grosnick, and T. D. S. Stanislaus  
100 *Valparaiso University, Valparaiso, Indiana 46383*

101 K. Gopal, C. Jena, R. Sharma, S. R. Sharma, and P. Sinha  
102 *Indian Institute of Science Education and Research (IISER) Tirupati, Tirupati 517507, India*

103 A. Hamed  
104 *American University of Cairo, New Cairo 11835, New Cairo, Egypt*

105 X. H. He, C. Hu, Q. Hu, S. Kumar, C. Liu, T. Lu, A. K. Pandey,  
106 H. Qiu, S. Singha, X. Sun, J. Wu, X. Zhang, Y. Zhang, and F. Zhao  
107 *Institute of Modern Physics, Chinese Academy of Sciences, Lanzhou, Gansu 730000*

108 J. Jia  
109 *Brookhaven National Laboratory, Upton, New York 11973 and*  
110 *State University of New York, Stony Brook, New York 11794*

111 X. Ju, C. Li, X. Li, Y. Li, Z. Li, M. Shao, K. Shen, F. Si, Y. Su,  
112 Y. Sun, Z. Tang, Y. Wang, W. Zha, S. Zhang, Y. Zhang, and J. Zhou  
113 *University of Science and Technology of China, Hefei, Anhui 230026*

114 D. Kalinkin  
115 *University of Kentucky, Lexington, Kentucky 40506-0055 and*  
116 *Brookhaven National Laboratory, Upton, New York 11973*

117 D. Mallick, B. Mohanty, and A. Pandav  
118 *National Institute of Science Education and Research, HBNI, Jatni 752050, India*

119 J. A. Mazer, T. Pani, D. Roy, and S. Salur

120 *Rutgers University, Piscataway, New Jersey 08854*

121 M. I. Nagy  
122 *ELTE Eötvös Loránd University, Budapest, Hungary H-1117*

123 R. L. Ray  
124 *University of Texas, Austin, Texas 78712*

125 N. Schmitz and P. Seyboth  
126 *Max-Planck-Institut für Physik, Munich 80805, Germany*

127 J. Seger and D. Tlustý  
128 *Creighton University, Omaha, Nebraska 68178*

129 N. Shah  
130 *Indian Institute Technology, Patna, Bihar 801106, India*

131 M. J. Skoby  
132 *Ball State University, Muncie, Indiana, 47306 and*  
133 *Purdue University, West Lafayette, Indiana 47907*

134 Y. Sun, J. S. Wang, and H. Xu  
135 *Huzhou University, Huzhou, Zhejiang 313000*

136 T. Tarnowsky and G. D. Westfall  
137 *Michigan State University, East Lansing, Michigan 48824*

138 O. D. Tsai  
139 *University of California, Los Angeles, California 90095 and*  
140 *Brookhaven National Laboratory, Upton, New York 11973*

141 C. Y. Tsang  
142 *Kent State University, Kent, Ohio 44242 and*  
143 *Brookhaven National Laboratory, Upton, New York 11973*

144 D. G. Underwood  
145 *Argonne National Laboratory, Argonne, Illinois 60439 and*  
146 *Valparaiso University, Valparaiso, Indiana 46383*

147 A. N. Vasiliev  
148 *NRC "Kurchatov Institute", Institute of High Energy Physics, Protvino 142281 and*  
149 *National Research Nuclear University MEPhI, Moscow 115409*

150 S. Yang  
151 *South China Normal University, Guangzhou, Guangdong 510631*

152 M. Zurek  
153 *Argonne National Laboratory, Argonne, Illinois 60439*

154 M. Zyzak  
155 *Frankfurt Institute for Advanced Studies FIAS, Frankfurt 60438, Germany*  
156 (STAR Collaboration)

157 We report here the first observation of directed flow ( $v_1$ ) of the hypernuclei  ${}^3_{\Lambda}\text{H}$  and  ${}^4_{\Lambda}\text{H}$  in mid-  
158 central Au+Au collisions at  $\sqrt{s_{NN}} = 3$  GeV at RHIC. These data are taken as part of the beam  
159 energy scan program carried out by the STAR experiment. From 165 million events in 5-40%  
160 centrality, about 8400  ${}^3_{\Lambda}\text{H}$  and 5200  ${}^4_{\Lambda}\text{H}$  candidates are reconstructed through two- and three-body  
161 decay channels. We observe that these hypernuclei exhibit significant directed flow. Comparing to

that of light nuclei, it is found that the mid-rapidity  $v_1$  slopes of  ${}^3_{\Lambda}\text{H}$  and  ${}^4_{\Lambda}\text{H}$  follow baryon number scaling, implying that the coalescence is the dominant mechanism for these hypernuclei production in the 3 GeV Au+Au collisions.

When a nucleon is replaced by a hyperon (*e.g.*  $\Lambda$ ,  $\Sigma$ ) with strangeness  $S = -1$ , a nucleus is transformed into a hypernucleus which allows for the study of the hyperon-nucleon ( $Y$ - $N$ ) interaction. It is well known that two-body  $Y$ - $N$  and three-body  $Y$ - $N$ - $N$  interactions, especially at high baryon density, are essential for understanding the inner structure of compact stars [1, 2]. New results on precision measurements of  $\Lambda$ - $p$  elastic scattering from Jefferson Lab [3] and  $\Sigma^-$ - $p$  elastic scattering from J-PARC [4, 5] became available recently, which may help to constrain the equation of state of high density matter inside a neutron star. Until recently, almost all hypernuclei measurements have been carried out with light particle (*e.g.*  $e$ ,  $\pi^+$ ,  $K^-$ ) induced reactions where the  $Y$ - $N$  interaction around the saturation density is analyzed from spectroscopic properties of hypernuclei.

Utilizing hypernuclei production in heavy-ion collisions to study the  $Y$ - $N$  interaction and the properties of QCD matter has been a subject of interest in the past decades [9–13]. However, due to limited statistics, measurements have been mainly focused on the light hypernuclei lifetime, binding energy and production yields [12, 14, 15]. Thermal model [16] and hadronic transport model with coalescence afterburner [17, 18] calculations have predicted abundant production of light hypernuclei in high-energy nuclear collisions, especially at high baryon density. Anisotropic flow has been commonly used for studying the properties of matter created in high energy nuclear collisions. Due to its genuine sensitivity to early collision dynamics [19–22], the first order coefficient of the Fourier-expansion of the azimuthal distribution in the momentum space,  $v_1$ , also called the directed flow, has been analyzed for many particles species ranging from  $\pi$ -mesons to light nuclei [23–28]. Collective flow is driven by pressure gradients created in such collisions. Hence, measurements of hypernuclei collectivity make it possible to study the  $Y$ - $N$  interactions in the QCD equation of state at high baryon density.

In this paper, we report the first observation of directed flow,  $v_1$ , of  ${}^3_{\Lambda}\text{H}$  and  ${}^4_{\Lambda}\text{H}$  in center-of-mass energy  $\sqrt{s_{\text{NN}}} = 3$  GeV Au+Au collisions. The data were collected by the STAR experiment at RHIC with the fixed-target (FXT) setup in 2018. A gold beam of energy 3.85 GeV/u is bombarded on a gold target of thickness 1% interaction length, located at the entrance of STAR’s Time-Projection Chamber (TPC) [29]. The TPC, which is the main tracking detector in STAR, is 4.2 m long and 4 m in diameter, positioned inside a 0.5 T solenoidal magnetic field along the beam direction. The collision vertex position of each event along the beam direction,  $V_z$ , is required to be within  $\pm 2$  cm of the target position. An additional requirement on the collision vertex position to

be within a radius  $r$  of less than 2 cm is imposed to eliminate background events from interactions with the beam pipe. Beam-Beam Counters (BBC) [30] and the Time of Flight (TOF) detector [31] are used to obtain the minimum bias (MB) trigger condition. After event selection, a total of  $2.6 \times 10^8$  MB events are used for further analysis.

The centrality is determined using the charged particle multiplicity distribution within the pseudo-rapidity region  $-2 < \eta < 0$  together with Monte Carlo (MC) Glauber calculations [32, 33]. The directed flow ( $v_1$ ) is measured with respect to the first-order event plane, determined by the Event Plane Detector (EPD) [34] which covers  $-5.3 < \eta < -2.6$  for the FXT setup. For this analysis, a relatively wide centrality range, 5-40%, is selected where both the event plane resolution and the hypernuclei yield are maximized. The event plane resolution in the centrality range is 40 – 75% [35]. Detailed information on the event plane resolution can be found in the Supplemental Material.

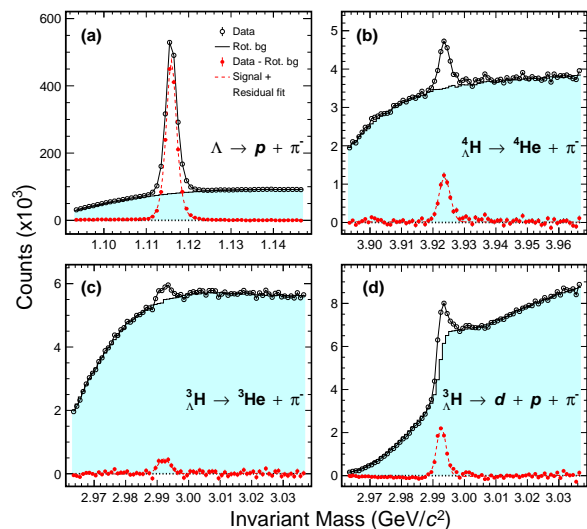


FIG. 1. Reconstructed  $\Lambda$  hyperon and hypernuclei invariant mass distributions from  $\sqrt{s_{\text{NN}}} = 3$  GeV Au+Au collisions in the corresponding  $p_T$ - $y$  regions listed in Table I. While top panels are for  $\Lambda \rightarrow p + \pi^-$  and  ${}^4_{\Lambda}\text{H} \rightarrow {}^4\text{He} + \pi^-$ , bottom panels represent the hypertriton two-body decay  ${}^3_{\Lambda}\text{H} \rightarrow {}^3\text{He} + \pi^-$  and three-body decay  ${}^3_{\Lambda}\text{H} \rightarrow d + p + \pi^-$ , respectively. Combinatorial backgrounds, shown as histograms, are constructed by rotating decay daughter particles. Background-subtracted invariant mass distributions are shown as filled circles.

In order to ensure high track quality, we require that the number of TPC points used in the track fitting (nHitsFit) to be larger than 15 (out of a maximum of 45).  ${}^3_{\Lambda}\text{H}$  is reconstructed via both two-body and three-

body decays  ${}^3_\Lambda\text{H} \rightarrow {}^3\text{He} + \pi^-$  and  ${}^3_\Lambda\text{H} \rightarrow d + p + \pi^-$  while  ${}^4_\Lambda\text{H}$  is reconstructed via the two-body decay channel,  ${}^4_\Lambda\text{H} \rightarrow {}^4\text{He} + \pi^-$ . Charged particles, including  $\pi^-$ ,  $p$ ,  $d$ ,  ${}^3\text{He}$  and  ${}^4\text{He}$  are selected based on the ionization energy loss ( $dE/dx$ ) measured in the TPC as a function of rigidity ( $p/|q|$ ), where  $p$  and  $q$  are the momentum and charge of the particle. The secondary decay topology is reconstructed using the KFParticle package based on a Kalman filter method [36, 37]. The package also utilizes the covariance matrix of reconstructed tracks to construct a set of topological variables. Selection cuts on these variables are placed on hypernuclei candidates to enhance the signal significance. Figure 1 shows the reconstructed invariant mass distributions for  $\Lambda$ ,  ${}^3_\Lambda\text{H}$  and  ${}^4_\Lambda\text{H}$  which are reconstructed using various decay channels the corresponding transverse momentum  $p_T$  - rapidity  $y$  regions as listed in Table I. Combinatorial background is estimated by rotating decay particles through a random angle between 10 and 350 degrees. For the  $\Lambda$ , the  $\pi^-$  is rotated. For the  ${}^3_\Lambda\text{H}$  two-body decay, the  ${}^3\text{He}$  is rotated, and for the  ${}^3_\Lambda\text{H}$  three-body decay, the deuteron is rotated. The combinatorial background, shown as shaded region, is normalized in the invariant mass region: (1.14, 1.16), (3.01, 3.04), and (3.95, 4.0)  $\text{GeV}/c^2$  for  $\Lambda$ ,  ${}^3_\Lambda\text{H}$  and  ${}^4_\Lambda\text{H}$ , respectively. The background-subtracted invariant mass distribution (filled circles) in each panel is fitted with a linear function plus a Student-t distribution for  $\Lambda$  and a Gaussian distribution for hypernuclei to extract the signal count. In total, 8400  ${}^3_\Lambda\text{H}$  and 5200  ${}^4_\Lambda\text{H}$  reconstructed hypernuclei from the 5-40% centrality bin are used for further analysis.

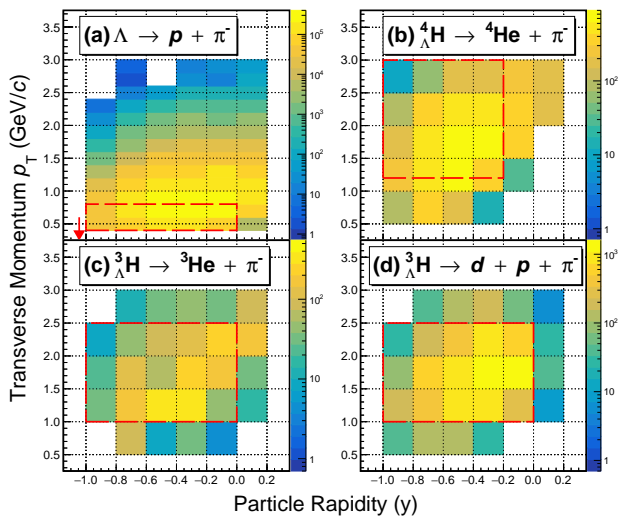


FIG. 2.  $\Lambda$  hyperon and hypernuclei acceptance, shown in  $p_T$  versus  $y$ , from the  $\sqrt{s_{\text{NN}}} = 3$  GeV Au+Au collisions. Dashed rectangular boxes illustrate the acceptance regions used for directed flow analysis, and the red arrow in panel a) represents the target rapidity ( $y_{\text{target}} = -1.045$ ).

TABLE I.  $p_T$ - $y$  acceptance windows of light nuclei,  $\Lambda$  hyperon and hypernuclei used for directed flow analysis.

Mass Number (A)	Particle	$p_T$ (GeV/c)	$y$
1	$\Lambda, p$	(0.4, 0.8)	(-1.0, 0.0)
2	$d$	(0.8, 1.6)	(-1.0, 0.0)
3	${}^3_\Lambda\text{H}$	(1.0, 2.5)	(-1.0, 0.0)
	$t, {}^3\text{He}$	(1.2, 2.4)	(-1.0, -0.1)
4	${}^4_\Lambda\text{H}$	(1.2, 3.0)	(-1.0, -0.2)
	${}^4\text{He}$	(1.6, 3.2)	(-1.0, -0.2)

structed  $\Lambda$ ,  ${}^3_\Lambda\text{H}$  and  ${}^4_\Lambda\text{H}$  candidates in the center-of-mass frame. Following the established convention [38], the negative sign is assigned to  $v_1$  in the rapidity region of  $y < 0$ . The  $p_T$ - $y$  acceptance windows used for our analysis are tabulated in Table I and also indicated in Fig. 2.

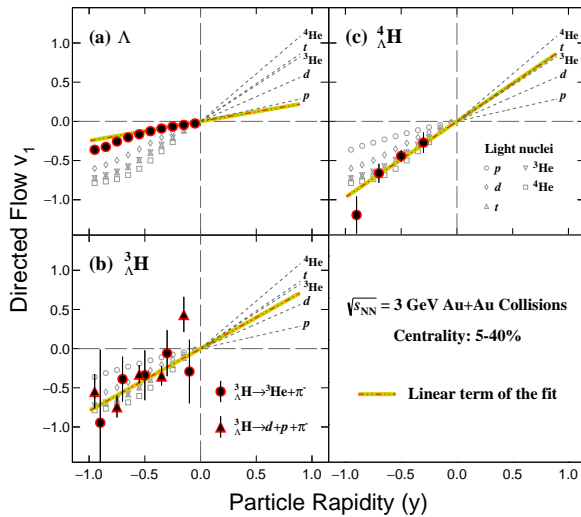
For  $p_T$ -integrated  $v_1$  measurements, the  $p_T$ -dependent reconstruction efficiency needs to be accounted for, which is estimated by the embedding method in STAR analyses [12, 39]. Monte-Carlo generated hyperons and hypernuclei are passed through the GEANT3 simulation of the STAR detector. The simulated TPC response is then embedded into data, and the whole event is processed and analyzed using the same procedure as in the data analysis. The two-dimensional reconstruction efficiency, including the detector acceptance, in  $p_T$ - $y$  are obtained for each decay channel, and applied to candidates in the data accordingly [40]. Kinematically, the three-body decay of  ${}^3_\Lambda\text{H}$  is very similar to the background of correlated  $d + \Lambda$  due to the very small  $\Lambda$  separation energy of  ${}^3_\Lambda\text{H}$ . Such correlated  $d + \Lambda$  pairs that pass the  ${}^3_\Lambda\text{H}$  three-body decay topological cuts are subtracted statistically (For details, see Fig. 3 in the Supplemental Material, which includes [41]). The  ${}^3_\Lambda\text{H}$  signal fraction within the invariant mass window (2.988, 2.998)  $\text{GeV}/c^2$  and rapidity range (-1.0, 0.0) is estimated to be  $0.69 \pm 0.03$ .

The directed flow of  $\Lambda$ ,  ${}^3_\Lambda\text{H}$  and  ${}^4_\Lambda\text{H}$  are extracted with the event plane method [42]. In each rapidity bin, the azimuthal angle with respect to the reconstructed event plane ( $\Phi = \Phi' - \Psi_1$ ) is further divided into four equal bins with a width of  $\pi/4$ , where  $\Phi'$  and  $\Psi_1$  are the azimuthal angle of a particle candidate and the first order event plane, respectively. After applying the reconstruction efficiency correction, the azimuthal angle distributions are fitted with a function  $f(\Phi) = c_0[1 + 2v_1^{obs} \cdot \cos(\Phi) + 2v_2^{obs} \cdot \cos(2\Phi)]$ , where  $c_0$ ,  $v_1^{obs}$  and  $v_2^{obs}$  are fitting parameters, and correspond to the normalization constant, the observed directed and the elliptic flow, respectively. To obtain the final  $v_1$  in a wide centrality range of 5-40% centrality in this analysis, the observed directed flow  $v_1^{obs}$  needs to be corrected for the average event plane resolution  $\langle 1/R \rangle$  [42], i.e  $v_1 = v_1^{obs} \cdot \langle 1/R \rangle$ , and  $\langle 1/R \rangle = \sum_i (N_i/R_i) / \sum_i N_i$ , where  $N_i$  and  $R_i$  stand for the number of particle candidates and the first order event plane resolution in the  $i$ -th centrality bin, respectively.

Figure 2 shows the  $p_T$  versus  $y$  acceptance of the recon-



318 The resulting  $\Lambda$  hyperon and hypernuclei  $v_1(y)$ , from<sup>346</sup>  
 319 5-40% mid-central Au+Au collisions at  $\sqrt{s_{NN}} = 3$  GeV<sup>347</sup>  
 320 , are shown in Fig. 3. For comparison, the  $v_1(y)$  of  $p$ ,<sup>348</sup>  
 321  $d$ ,  $t$ ,  ${}^3\text{He}$  and  ${}^4\text{He}$  from the same data [43] are shown as<sup>349</sup>  
 322 open symbols.  $v_1(y)$  of  $\Lambda$ ,  $p$ ,  $d$ ,  $t$ ,  ${}^3\text{He}$  and  ${}^4\text{He}$  are fitted<sup>350</sup>  
 323 with a third-order polynomial function  $v_1(y)=a\cdot y+b\cdot y^3$ <sup>351</sup>  
 324 in the rapidity ranges listed in Table I, where  $a$ , which  
 325 stands for the mid-rapidity slope  $dv_1/dy|_{y=0}$ , and  $b$  are  
 326 fitting parameters. Due to limited statistics, the hyper-  
 327 nuclei  $v_1(y)$  distributions are fitted with a linear function  
 328  $v_1(y)=a\cdot y$ , in the rapidity range  $-1.0 < y < 0.0$ . The linear  
 329 terms for light nuclei are plotted as dashed lines in the  
 330 positive rapidity region, while for  $\Lambda$ ,  ${}^3_\Lambda\text{H}$  and  ${}^4_\Lambda\text{H}$ , they  
 331 are shown by the yellow-red lines in the corresponding  
 332 panels. The  $\Lambda$  result is close to that of the proton, and  
 333 hypernuclei  $v_1(y)$  distributions are also similar to those  
 334 light nuclei with the same mass numbers. This is the  
 335 first observation of significant hypernuclei directed flow  
 336 in high-energy nuclear collisions.



337 FIG. 3.  $\Lambda$  hyperon and hypernuclei directed flow  $v_1$ , shown  
 338 as a function of rapidity, from the  $\sqrt{s_{NN}} = 3$  GeV 5-40%  
 339 mid-central Au+Au collisions. In the case of  ${}^3_\Lambda\text{H}$   $v_1$ , both  
 340 two-body (dots) and three-body (triangles) decays are used.  
 341 The linear terms of the fitting for  $\Lambda$ ,  ${}^3_\Lambda\text{H}$  and  ${}^4_\Lambda\text{H}$  are shown  
 342 as the yellow-red lines. The rapidity dependence of  $v_1$  for  $p$ ,  
 343  $d$ ,  $t$ ,  ${}^3\text{He}$ , and  ${}^4\text{He}$  are also shown as open markers (circles,  
 344 diamonds, up-triangles, down-triangles and squares), and the  
 345 linear terms of the fitting results are shown as dashed lines in<sup>352</sup>  
 the positive rapidity region [43].<sup>353</sup>  
<sup>354</sup>

337 Systematic uncertainties are estimated by varying<sup>355</sup>  
 338 track selection criteria for particle identification, as well<sup>356</sup>  
 339 as cuts on the topological variables used in the KFPAr-<sup>357</sup>  
 340 ticle package [36]. Major contributors to the systematic<sup>358</sup>  
 341 uncertainty are listed in Table II. As one can see, the<sup>359</sup>  
 342 dominant sources of systematic uncertainty are from hy-<sup>360</sup>  
 343 pernuclei candidate selection, estimated by varying topo-<sup>361</sup>  
 344 logical cuts and nHitsFit. Event plane resolution de-<sup>362</sup>  
 345 termination also contributes 1.4% [40]. Assuming these<sup>363</sup>

sources are uncorrelated, the total systematic uncertainty  
 is obtained by adding them together quadratically. In  
 case of the  ${}^3_\Lambda\text{H}$  three-body decay, the fraction of the cor-  
 related  $d\Lambda$  contamination has been analyzed in each rap-  
 idity bin. Its systematic uncertainty contribution to the  
 final  $v_1$  slope is negligible.

TABLE II. Sources of systematic uncertainties for mid-  
 rapidity slope  $dv_1/dy|_{y=0}$  of  ${}^3_\Lambda\text{H}$  and  ${}^4_\Lambda\text{H}$ .

Source	${}^3_\Lambda\text{H}$		${}^4_\Lambda\text{H}$
	two-body	three-body	two-body
Topological cuts	1.3%	9.4%	8.0%
nHitsFit	9.0%		<1.0%
EP Resolution	1.4%		1.4%
Total	13.1%		8.3%

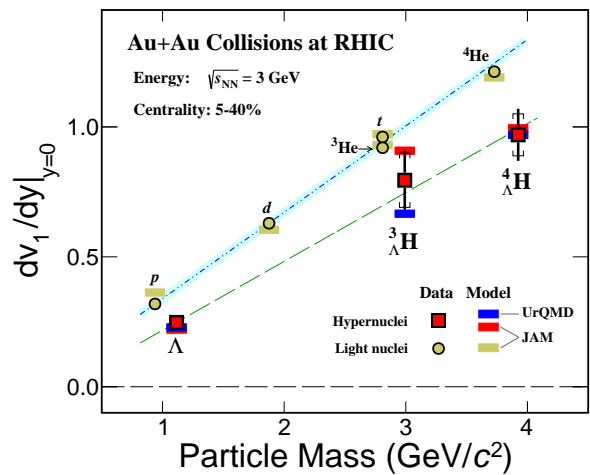


FIG. 4. Mass dependence of the mid-rapidity  $v_1$  slope,  
 $dv_1/dy$ , for  $\Lambda$ ,  ${}^3_\Lambda\text{H}$  and  ${}^4_\Lambda\text{H}$  from the  $\sqrt{s_{NN}} = 3$  GeV 5-40%  
 mid-central Au+Au collisions. The statistical and system-  
 atic uncertainties are presented by vertical lines and square  
 brackets, respectively. The slopes of  $p$ ,  $d$ ,  $t$ ,  ${}^3\text{He}$  and  ${}^4\text{He}$   
 from the same collisions are shown as black circles. The blue  
 and dashed green lines are the results of a linear fit to the  
 measured light nuclei and hypernuclei  $v_1$  slopes, respectively.  
 For comparison, calculations of transport models plus coalescence  
 afterburner are shown as gold and red bars from JAM model,  
 and blue bars from UrQMD model.

The results of the mid-rapidity slope  $dv_1/dy$  for  $\Lambda$ ,  ${}^3_\Lambda\text{H}$   
 (both two- and three-body decays) and  ${}^4_\Lambda\text{H}$  are shown in  
 Fig. 4, as filled squares, as a function of particle mass.  
 For comparison,  $v_1$  slopes of  $p$ ,  $d$ ,  $t$ ,  ${}^3\text{He}$  and  ${}^4\text{He}$   
 from the same 5-40%  $\sqrt{s_{NN}} = 3$  GeV Au+Au collisions are  
 shown as open circles. The  $\Lambda$  hyperon and hypernuclei  
 slopes  $dv_1/dy$  are all systematically lower than the nuclei  
 of same mass numbers. Linear fits ( $f = a + b\cdot\text{mass}$ ) are  
 performed on the mass dependence of  $dv_1/dy$  for both  
 light nuclei and hypernuclei. For light nuclei, only statisti-  
 cal uncertainties are used in the fit, while statistical and  
 systematic uncertainties are used for hypernuclei. The

slope parameters  $b$  are  $0.3323 \pm 0.0003$  for light nuclei and  $0.27 \pm 0.04$  for hypernuclei. As one can see, their slopes are similar within uncertainties.

Using transport models JAM [22, 44] and UrQMD [21],  $v_1(y)$  of  $\Lambda$  and hypernuclei are simulated for the 3 GeV Au+Au collisions within the same centrality and kinematic acceptance used in data analysis. For comparison, similar calculations are performed for light nuclei. The simulation is done in two steps: (i) using JAM model (with momentum-dependent potential) and UrQMD model (without momentum-dependent potential) in the mean field mode with the incompressibility  $\kappa = 380$  MeV to produce neutrons, protons and  $\Lambda$ s at kinetic freeze-out; (ii) forming hypernuclei through the coalescence of  $\Lambda$  and nucleons, similar to the light nuclei production with the coalescence procedure discussed in [43]. The probability for hypernuclei production is dictated by coalescence parameters of relative momenta  $\Delta p < 0.12$  (0.3) GeV/itc and relative distance  $\Delta r < 4$  fm in the rest frame of  $np\Lambda$  ( $nnp\Lambda$ ) for  ${}^3_\Lambda\text{H}$  ( ${}^4_\Lambda\text{H}$ ). These parameters are chosen such that the hypernuclei yields at mid-rapidity can be described [12]. The rapidity dependences of  $v_1$  from the model calculations are then fitted with a third-order polynomial function within the rapidity interval  $-1.0 \leq y \leq 0.0$ . The resulting mid-rapidity slopes are shown in Fig. 4 as red and blue bars for JAM and UrQMD models, respectively. In the figure, results for light nuclei from JAM are also presented as gold bars.

Both transport models (JAM and UrQMD) plus coalescence afterburner calculations for hypernuclei are in agreement with data within uncertainties. Interactions among baryons and strange baryons are important in gradients in the transport models, especially in the high baryon density region [45, 46]. The properties of the medium is determined by such interactions. In addition, the yields of hypernuclei, if created via the coalescence process, are also strongly affected by the hyperon and nucleon interactions. In our treatment, the coalescence parameters used ( $\Delta r$ ,  $\Delta p$ ) reflect the production probability determined by  $N$ - $N$  and  $Y$ - $N$  interactions [18, 47, 48]. The mass dependence of the  $v_1(y)$  slope implies that coalescence might be the dominant mechanism for hypernuclei production in such heavy-ion collisions. The mass dependence of the hypernuclei  $v_1$  slope also seems to be similar to that of light nuclei, as shown in Fig. 4, although it may not necessarily be so due to the differences in  $N$ - $N$  and  $Y$ - $N$  interactions. Clearly, precision data on hypernuclei collectivity will yield invaluable insights on  $Y$ - $N$  interactions at high baryon density.

This is the first report of the collectivity of hypernuclei in heavy-ion collisions. Hydrodynamically, collective motion is driven by pressure gradients created in such collisions. This work opens up a new direction for studying  $Y$ - $N$  interaction under finite pressure [49]. This is important for making connection between nuclear collisions and the equation of state which governs the inner

structure of compact stars.

To summarize, we report the first observation of hypernuclei  ${}^3_\Lambda\text{H}$  and  ${}^4_\Lambda\text{H}$   $v_1$  from  $\sqrt{s_{\text{NN}}} = 3$  GeV mid-central 5-40% Au+Au collisions at RHIC. The rapidity dependences of their  $v_1$  are compared with those of  $\Lambda$ ,  $p$ ,  $d$ ,  $t$ ,  ${}^3\text{He}$  and  ${}^4\text{He}$  in the same collisions. It is found that, within uncertainties, the mass dependent  $v_1$  slope of hypernuclei,  ${}^3_\Lambda\text{H}$  and  ${}^4_\Lambda\text{H}$  is similar to that of light nuclei, implying that they follow the baryon mass scaling. Calculations from transport models (JAM and UrQMD) plus coalescence afterburner can qualitatively reproduce the rapidity dependence of  $v_1$  and the mass dependence of  $v_1$  slope. These observations suggest that coalescence of nucleons and hyperon  $\Lambda$  could be the dominant mechanism for the hypernuclei  ${}^3_\Lambda\text{H}$  and  ${}^4_\Lambda\text{H}$  production in the 3 GeV collisions. Model calculations suggest that baryon density at freeze-out may depend on collision energy [50–52]. High statistics data at different energies, especially at the high baryon density region, will help in extracting the information on  $Y$ - $N$  interaction and possibly its density dependence in the future.

**Acknowledgments:** We thank Drs. Y. Nara and J. Steinheimer for insightful discussions. We thank the RHIC Operations Group and RCF at BNL, the NERSC Center at LBNL, and the Open Science Grid consortium for providing resources and support. This work was supported in part by the Office of Nuclear Physics within the U.S. DOE Office of Science, the U.S. National Science Foundation, National Natural Science Foundation of China, Chinese Academy of Science, the Ministry of Science and Technology of China and the Chinese Ministry of Education, the Higher Education Sprout Project by Ministry of Education at NCKU, the National Research Foundation of Korea, Czech Science Foundation and Ministry of Education, Youth and Sports of the Czech Republic, Hungarian National Research, Development and Innovation Office, New National Excellence Programme of the Hungarian Ministry of Human Capacities, Department of Atomic Energy and Department of Science and Technology of the Government of India, the National Science Centre and WUT ID-UB of Poland, the Ministry of Science, Education and Sports of the Republic of Croatia, German Bundesministerium für Bildung, Wissenschaft, Forschung und Technologie (BMBF), Helmholtz Association, Ministry of Education, Culture, Sports, Science, and Technology (MEXT) and Japan Society for the Promotion of Science (JSPS).

- 
- [1] D. Gerstung, N. Kaiser, and W. Weise, Eur. Phys. J. A **56**, 175 (2020), arXiv:2001.10563 [nucl-th].
  - [2] D. Lonardonì, A. Lovato, S. Gandolfi, and F. Pederiva, Phys. Rev. Lett. **114**, 092301 (2015), arXiv:1407.4448 [nucl-th].
  - [3] J. Rowley *et al.* (CLAS), Phys. Rev. Lett. **127**, 272303

- (2021), arXiv:2108.03134 [hep-ex]. 525
- [4] K. Miwa *et al.* (J-PARC E40), Phys. Rev. C **104**, 045204 (2021), arXiv:2104.13608 [nucl-ex]. 527
- [5] K. Miwa *et al.* (J-PARC E40), Phys. Rev. Lett. **128**, 072501 (2022), arXiv:2111.14277 [nucl-ex]. 529
- [6] A. Gal, E. V. Hungerford, and D. J. Millener, Rev. Mod. Phys. **88**, 035004 (2016), arXiv:1605.00557 [nucl-th]. 531
- [7] O. Hashimoto and H. Tamura, Prog. Part. Nucl. Phys. **57**, 564 (2006). 533
- [8] L. Tang *et al.* (HKS), Phys. Rev. C **90**, 034320 (2014), arXiv:1406.2353 [nucl-ex]. 534
- [9] B. I. Abelev *et al.* (STAR), Science **328**, 58 (2010), arXiv:1003.2030 [nucl-ex]. 536
- [10] S. Acharya *et al.* (ALICE), Phys. Lett. B **797**, 134905 (2019), arXiv:1907.06906 [nucl-ex]. 538
- [11] L. Adamczyk *et al.* (STAR), Phys. Rev. C **97**, 054909 (2018), arXiv:1710.00436 [nucl-ex]. 540
- [12] M. Abdallah *et al.* (STAR), Phys. Rev. Lett. **128**, 202301 (2022), arXiv:2110.09513 [nucl-ex]. 542
- [13] T. R. Saito *et al.*, Nature Rev. Phys. **3**, 803 (2021). 544
- [14] J. Chen, D. Keane, Y.-G. Ma, A. Tang, and Z. Xu, Phys. Rept. **760**, 1 (2018), arXiv:1808.09619 [nucl-ex]. 545
- [15] J. Adam *et al.* (STAR), Nature Phys. **16**, 409 (2020), arXiv:1904.10520 [hep-ex]. 547
- [16] A. Andronic, P. Braun-Munzinger, J. Stachel, and H. Stöcker, Phys. Lett. B **697**, 203 (2011), arXiv:1010.2995 [nucl-th]. 549
- [17] J. Steinheimer *et al.*, Phys. Lett. B **714**, 85 (2012), arXiv:1203.2547 [nucl-th]. 550
- [18] J. Aichelin *et al.*, Phys. Rev. C **101**, 044905 (2020), arXiv:1907.03860 [nucl-th]. 552
- [19] C. M. Hung and E. V. Shuryak, Phys. Rev. Lett. **75**, 4003 (1995), arXiv:hep-ph/9412360. 554
- [20] J. Brachmann *et al.*, Phys. Rev. C **61**, 024909 (2000), arXiv:nucl-th/9908010. 555
- [21] J. Steinheimer, J. Auvinen, H. Petersen, M. Bleicher, and H. Stöcker, Phys. Rev. C **89**, 054913 (2014), arXiv:1402.7236 [nucl-th]. 556
- [22] Y. Nara, H. Niemi, A. Ohnishi, and H. Stöcker, Phys. Rev. C **94**, 034906 (2016), arXiv:1601.07692 [hep-ph]. 562
- [23] L. Adamczyk *et al.* (STAR), Phys. Rev. Lett. **112**, 162301 (2014), arXiv:1401.3043 [nucl-ex]. 564
- [24] L. Adamczyk *et al.* (STAR), Phys. Rev. Lett. **120**, 062301 (2018), arXiv:1708.07132 [hep-ex]. 565
- [25] J. Adam *et al.* (STAR), Phys. Rev. C **102**, 044906 (2020), arXiv:2007.04609 [nucl-ex]. 567
- [26] L. Adamczyk *et al.* (STAR), Phys. Rev. C **88**, 014902 (2013), arXiv:1301.2348 [nucl-ex]. 570
- [27] J. Adam *et al.* (STAR), Phys. Rev. C **103**, 034908 (2021), arXiv:2007.14005 [nucl-ex]. 572
- [28] A. Bzdak *et al.*, Phys. Rept. **853**, 1 (2020), arXiv:1906.00936 [nucl-th]. 573
- [29] M. Anderson *et al.*, Nucl. Instrum. Meth. A **499**, 659 (2003), arXiv:nucl-ex/0301015. 525
- [30] C. A. Whitten (STAR), AIP Conf. Proc. **980**, 390 (2008). 527
- [31] W. J. Llope (STAR), Nucl. Instrum. Meth. A **661**, S110 (2012). 529
- [32] M. L. Miller, K. Reygers, S. J. Sanders, and P. Steinberg, Ann. Rev. Nucl. Part. Sci. **57**, 205 (2007), arXiv:nucl-ex/0701025. 530
- [33] B. I. Abelev *et al.* (STAR), Phys. Rev. C **81**, 024911 (2010), arXiv:0909.4131 [nucl-ex]. 531
- [34] J. Adams *et al.*, Nucl. Instrum. Meth. A **968**, 163970 (2020), arXiv:1912.05243 [physics.ins-det]. 532
- [35] M. S. Abdallah *et al.* (STAR), Phys. Lett. B **827**, 137003 (2022), arXiv:2108.00908 [nucl-ex]. 533
- [36] I. Kisel (CBM), J. Phys. Conf. Ser. **1070**, 012015 (2018). 534
- [37] M. Zyzak, *Online selection of short-lived particles on many-core computer architectures in the CBM experiment at FAIR*, Ph.D. thesis, Frankfurt U. (2016). 535
- [38] H. Liu *et al.* (E895), Phys. Rev. Lett. **84**, 5488 (2000), arXiv:nucl-ex/0005005. 536
- [39] J. Adam *et al.* (STAR), Phys. Rev. C **102**, 034909 (2020), arXiv:1906.03732 [nucl-ex]. 537
- [40] M. S. Abdallah *et al.* (STAR), Phys. Lett. B **827**, 137003 (2022), arXiv:2108.00908 [nucl-ex]. 538
- [41] J. Haidenbauer, Phys. Rev. C **102**, 034001 (2020), arXiv:2005.05012 [nucl-th]. 539
- [42] H. Masui, A. Schmah, and A. M. Poskanzer, Nucl. Instrum. Meth. A **833**, 181 (2016), arXiv:1212.3650 [physics.data-an]. 540
- [43] M. Abdallah *et al.* (STAR), Phys. Lett. B **827**, 136941 (2022), arXiv:2112.04066 [nucl-ex]. 541
- [44] Y. Nara *et al.*, Phys. Rev. C **61**, 024901 (2000), arXiv:nucl-th/9904059. 542
- [45] A. S. Botvina, K. K. Gudima, J. Steinheimer, M. Bleicher, and J. Pochodzalla, Phys. Rev. C **95**, 014902 (2017), arXiv:1608.05680 [nucl-th]. 543
- [46] A. S. Botvina, J. Steinheimer, E. Bratkovskaya, M. Bleicher, and J. Pochodzalla, Phys. Lett. B **742**, 7 (2015), arXiv:1412.6665 [nucl-th]. 544
- [47] T. Shao, J. Chen, C. M. Ko, K.-J. Sun, and Z. Xu, Chin. Phys. C **44**, 114001 (2020), arXiv:2004.02385 [nucl-ex]. 545
- [48] F. Wang and S. Pratt, Phys. Rev. Lett. **83**, 3138 (1999), arXiv:nucl-th/9907019. 546
- [49] T. Neidig, K. Gallmeister, C. Greiner, M. Bleicher, and V. Vovchenko, Phys. Lett. B **827**, 136891 (2022), arXiv:2108.13151 [hep-ph]. 547
- [50] T. Reichert, G. Inghirami, and M. Bleicher, Eur. Phys. J. A **56**, 267 (2020), arXiv:2007.06440 [nucl-th]. 548
- [51] J. Cleymans, H. Oeschler, K. Redlich, and S. Wheaton, Phys. Rev. C **73**, 034905 (2006), arXiv:hep-ph/0511094. 549
- [52] J. Randrup and J. Cleymans, Phys. Rev. C **74**, 047901 (2006), arXiv:hep-ph/0607065. 550